Dietary sulfur amino acid restriction elicits a cold-like transcriptional response in inguinal but not epididymal white adipose tissue of male mice

Philip M.M. Ruppert[1], Aylin S. Güller[1], Marcus Rosendal[1], Natasa Stanic[1], Jan-Wilhelm Kornfeld[1,2]

[1]Functional Genomics and Metabolism Unit, Department for Biochemistry and Molecular Biology, University of Southern Denmark, Odense, Denmark
[2]Novo Nordisk Foundation Center for Adipocyte Signaling, University of Southern Denmark, Odense, Denmark

Keywords: Physiology, non-shivering thermogenesis, transcriptomics, thermoregulation, amino acid metabolism, adipose tissue

Correspondence should be addressed to:
Professor Jan-Wilhelm Kornfeld, Dr. rer. nat.
Department of Molecular Biology
University of Southern Denmark
Campusvej 55
DK-5230 Odense M
Email: janwilhelmkornfeld@bmb.sdu.dk
Telephone: +45 9350 7481

Author contributions experiments/analysis:
PMMR: Mouse experiments, Indirect Calorimetry, RNA isolation, NGS analysis, ELISA
MR: ELISA
ASG: Tissue preparation, RNA isolation, ELISA
NS: Mouse experiments, tissue preparation

Abstract

Introduction: About 1 billion people are living with obesity worldwide. GLP-1-based drugs have massively transformed care, but long-term consequences are unclear in part due to reductions in energy expenditure with ongoing use. Diet-induced thermogenesis (DIT) and cold exposure (CE) raise EE via brown adipose tissue (BAT) activation and beiging of white adipose tissue (WAT). Methionine restriction (MetR) is a candidate DIT trigger, but its EE effect has not been benchmarked against CE, nor have their tissue-level interactions been defined.

Objective & Methods: In a 2×2 design (Control vs. MetR; room temperature, RT: 22 °C vs. CE: 4 °C for 24 h), we used male C57BL/6N mice to benchmark MetR-induced thermogenesis against CE and mapped how diet and temperature interact across tissues. Bulk RNA-seq profiled liver, iBAT, iWAT, and eWAT. Differential expression was modeled with main effects and a diet×temperature interaction; KEGG GSEA assessed pathways.

Results: MetR increased EE at RT and shifted fuel use toward lipid oxidation, supporting MetR as a bona fide DIT factor. CE elevated EE across diets and blunted diet differences. Transcriptomic responses were tissue-specific: in liver, CE dominated gene induction while MetR and CE cooperatively repressed genes. The combination enriched glucagon/AMPK-linked and core metabolic pathways. In iBAT, CE dominated thermogenic and lipid-oxidation programs with minimal MetR contribution. In iWAT, MetR and CE acted largely additively with high concordance, enhancing fatty-acid degradation, PPAR signaling, thermogenesis, and TCA cycle pathways. In eWAT, robust co-dependent differential expression emerged only with MetR+CE, yet pathway-level enrichment was limited.

Conclusion: MetR is a genuine DIT stimulus that remodels metabolism in a tissue-specific manner. Our study provides a tissue-resolved transcriptomic resource that benchmarks diet-induced (MetR) against cold-induced thermogenesis and maps their interactions across liver, iBAT, iWAT, and eWAT.

Introduction

Obesity has become a global health crisis, with prevalence rates reaching alarming levels in many countries. The World Health Organization (WHO) estimates that over 890 million adults worldwide are obese (1), leading to a dramatic increase in obesity-related diseases such as type 2 diabetes, cardiovascular disease, and certain cancers. As traditional weight-loss strategies often fail to provide lasting results, new therapeutic approaches are urgently needed. The increase in energy expenditure via brown adipose tissue (BAT) activation has emerged as a promising strategy for combating obesity. Unlike white adipose tissue (WAT), which stores excess energy, BAT is specialized in generating heat and driving energy expenditure via non-shivering-thermogenesis, typically in response to cold exposure (CE). Pharmacological or environmentally induced BAT activity results in improved metabolic health in mice and humans (2,3). Conversely, diet-induced thermogenesis (DIT) refers to the increase in energy expenditure associated with the digestion, absorption, and metabolism of food.

Recent studies have suggested that sulfur amino acid restriction, also referred to as Methionine restriction (MetR), a dietary intervention that limits the intake of the amino acids Methionine and Cysteine, can enhance energy expenditure (EE) and promote metabolic health (4). Methionine and Cysteine are amino acids involved in a plethora of metabolic reactions including protein synthesis, gene expression via methylation of DNA and histones, maintenance of DNA and RNA integrity via polyamine synthesis, redox balance via glutathione and H_2S metabolism, and nucleotide biosynthesis via the folate cycle (4,5). Recent studies have shown that DIT via dietary MetR augments energy expenditure in a UCP1-dependent and temperature-independent fashion (6). Mechanistically, MetR is sensed in the liver by the GCN2-PERK-ATF4-mediated integrated stress response, which results in the secretion of FGF21. In turn, FGF21 augments EE by activating UCP1-driven thermogenesis in brown adipose tissue via beta-adrenergic (βr) signaling (4,7), although some metabolic benefits develop in βr-incompetent, FGF21-KO or UCP1-KO animals (5,6,8).

Above-mentioned studies highlight an intriguing overlap between diet- and cold-induced thermogenesis, particularly in the context of energy expenditure regulation. Both stimuli rely on the activation of brown adipose tissue (BAT) and the ‘beiging’ of inguinal white adipose tissue (iWAT) to promote UCP1 expression and increase mitochondrial activity, and thereby boost calorie dissipation, potentially via similar signaling pathways, including the

sympathetic nervous system and key metabolic regulators like FGF21 (9). However, whether diet- and cold-induced thermogenesis produce additive or synergistic effects on the activation of energy and systemic metabolism is unknown. Here, we systematically compare the physiological and transcriptional responses to MetR and CE across multiple metabolically active tissues. Using RNA-sequencing, we dissect additive, synergistic, and antagonistic gene regulatory patterns, and assess whether combining MetR with CE produces tissue-specific concordant or discordant novel transcriptional outcomes.

We demonstrate that MetR increased EE at RT and shifted fuel use toward lipid oxidation. CE elevated EE across diets and blunted diet differences. The transcriptional responses were tissue-specific on gene and pathway level. Taken together, our results provide a unique and comprehensive gene regulatory framework to understand how dietary and environmental cues converge to shape tissue-specific gene expression programs and metabolic adaptation.

Materials & Methods:

All animal experiments were performed in accordance with the Directive 2010/63/EU from the European Union and approved by the Ministry of Environment and Agriculture Denmark (Miljø- og Fødevarestyrelsen) under license no. 2018-15-0201-01544.

Animal husbandry & experiments

All experiments were performed in male mice on a C57Bl/6N background (Taconic, Denmark). All mice were housed under a 12-hour light/dark cycle in a temperature and humidity-controlled facility and had ad libitum access to diets and drinking water. 8/9-week-old were acclimatized to our animal facility on a chow diet (NIH-31, Zeigler Brothers Inc., 8% calories from fat) and housed in groups of 3-4 animals per cage for the habituation period. For reproducibility reasons and to avoid biases by 'social thermogenesis' we single-housed all mice for the duration of the experiments and concluded the experiments with mice being 16 weeks of age.

In study 1 we performed indirect calorimetry to assess physiological effects and interactions between diets and ambient temperature. For this 15 mice were split randomly into 3 groups and fed cysteine-depleted diets containing either 0.8% Methionine (Control; Ctrl), 0.12% Methionine (Methionine-restricted; MetR) or 2% Methionine (Methionine-supplemented; MetS) for 6 days at 22ºC and 5 days at 4ºC. Diets were from Research diets (New Brunswick, NJ, USA). Exact compositions can be retrieved under cat.no. A11051301B (MetR), A11051302B (Ctrl) and A21060801 (MetS).

In study 2, we performed detailed analyses of physiological (body and organ weights) and molecular parameters (RNA-seq, colorimetric/enzymatic assays) to investigate the molecular adaptations and interactions between diet and temperature. For this 28 mice were split randomly into 4 groups and were either fed previously mentioned Ctrl or MetR diets at 22ºC for 7 days or housed an additional 8th day at 4 ºC. Blood glucose were determined just prior to sacrifice in the cage using a standard glucometer . The mice were then euthanized by carbon dioxide asphyxiation followed by cervical dislocation. Blood was collected by cardiac puncture and stored on ice for the duration of the sacrifice. Serum was collected after centrifugation by 2,000 g for 15 min and stored at -80 °C. Mice were sacrificed by carbon dioxide euthanasia. Liver, eWAT, iWAT and BAT were weighed and snap-frozen in liquid nitrogen and then stored at -80 °C.

Indirect calorimetry

Indirect calorimetry was conducted using the PhenoMaster NG 2.0 Home Cage System (TSE systems, Bad Homburg, Germany). Prior to the experiment, a complete calibration protocol for the gasanalysers was run according to the manufacturer's recommendations, and the mice were weighed. Mice were housed individually and acclimated to the new environment for 3 days prior to the experiment. The machine was set to maintain 50% humidity throughout the experiment and a 12-hour light/dark cycle, with ad libitum access to food and water. During the experiment energy expenditure, respiratory exchange ratio, food and water intake were recorded every 60 seconds and datapoints were filtered for outliers and then averaged per hour for the analysis. Indirect calorimetry data are presented as mean ± SEM.

RNA sequencing and analysis

Total RNAs from tissues were isolated using the TRI reagent (Sigma) followed by clean-up with RPE buffer (Qiagen, Germany). The quality of RNA was validated by the Agilent RNA 6000 Nano-Kit in Agilent 2100 Bioanalyzer according to the manufacturer's protocol (Agilent Technologies, Waldbronn, Germany). mRNA sequencing was performed in-house. After quality control 500 ng RNA in a final volume of 25 µL DEPC-treated water was prepared and sample preparation was performed as described in the NEBNext Poly(A) mRNA Magnetic Isolation Module kit and NEBNext Ultra II RNA Library Prep Kit (cat no: #E7770, New England Biolabs, Ipswich, MA, USA). The amplified libraries were validated by Agilent 2100 Bioanalyzer using a DNA 1000 kit (Agilent Technologies, Inc., Santa Clara, CA, USA) and quantified by qPCR using the KaPa Library Kits (KaPa Biosystems, Wilmington, MA, USA). Hereafter, 2x50bp paired-end sequencing was performed on Illumina Novaseq 6000.

RNAseq data analysis

Sequencing reads were aligned to the mouse reference genome (Gencode vM25) (10) using STAR aligner (v2.7.9a) (11) with the following parameters: --outSAMunmapped Within, --outFilterType BySJout, --outSAMattributes NH HI AS NM MD, --outFilterMultimapNmax 10, --outFilterMismatchNoverReadLmax 0.04, --alignIntronMin 20, --alignIntronMax 1000000, --alignMatesGapMax 1000000, --alignSJoverhangMin 8, and --alignSJDBoverhangMin 1. Gene-level quantification was performed using featureCounts (v2.0.3) (12). In parallel, transcript-level quantification was performed using Salmon (v1.9.0) (13) and Gencode vM25, with parameters --seqBias, --useVBOpt, and --numBootstraps 30. Transcript abundance estimates were imported and summarized to the gene level using the

tximport package (14). Differential gene expression analysis was performed using DESeq2 (v1.46.0) (15) with shrinkage of fold-changes using apeglm (16). Genes with fewer than 10 total counts across all samples were excluded prior to normalization. The following interaction model was applied: ~ diet + temperature + diet:temperature, allowing detection of diet effects, temperature effects, and their statistical interaction. Specifically, the model tested: (i) the main effect of diet (MetR vs. Ctrl), (ii) the main effect of temperature (CE vs. RT), and (iii) the diet × temperature interaction (whether the effect of MetR differs between RT and CE). Genes with an adjusted p-value < 0.05 and an absolute $\log_2 FC \geq 0.585$ were considered significantly differentially expressed. Gene set enrichment analysis (GSEA) was performed using the gseKEGG() function from the clusterProfiler package (v4.14.6) (17) with parameters: organism = "mmu", pvalueCutoff = 1, pAdjustMethod = "BH", minGSSize = 0, seed = TRUE, and eps = 0. Quality control metrics and preprocessing approaches were done as previously described (18).

Data availability

The RNA-seq data generated in this study have been deposited in the NCBI Gene Expression Omnibus (GEO) under accession number GSEXXXXXX. The dataset includes raw FASTQ files, processed count matrices, and metadata for all experimental conditions.

Serum measurements

Serum NEFA's were determined using the NEFA-HR(2) kit (cat. no. 434-91795 and 436-91995; FUJIFILM Wako Chemicals Europe GmbH). Serum triglycerides were determined using the LabAssay Triglyceride kit (cat no. 291-94501; FUJIFILM Wako Chemicals Europe GmbH). Serum beta-hydroxybutyrate levels were determined using the β-HBA kit (cat. no. 2940; Instruchemie, Delfzijl, the Netherlands). Serum FGF21 and IL-6 levels were determined using the Luminex Multiplex platform (R&D Systems).

Statistics

Statistical analysis of the transcriptomics data was performed as described in the previous paragraph. Serum, body and organ weight data were analyzed using GraphPad Prism (v. 10.4.1). Prior to the analysis, the assumptions of normality and homogeneity of variance were assessed. These assumptions were met in all presented parameters. Plasma parameters, absolute and relative organ weights and bodyweight change (%) were analyzed using an unpaired one-way ANOVA with Tukey's HSD test to correct for multiple comparisons.

Statistical differences between the groups were depicted in a compact letter display, were groups with the same letter are not significantly different and groups with different letters are significantly different. Bodyweight data (start/finished) and average daily locomotor activity and food and water intake (RT/CE) were analyzed using a paired two-way ANOVA with Tukey's HSD test to correct for multiple comparisons. Statistical differences between the groups were depicted as * $p < 0.05$, ** $p < 0.01$, *** $p < 0.001$, **** $p < 0.0001$. Energy expenditure, food and water intake data from the indirect calorimetry experiment was analyzed by ANCOVA with bodyweight or locomotor activity as covariate. The ANCOVA analysis was done pairwise using the regression tool at by NIDDK Mouse Metabolic Phenotyping Centers (MMPC, www.mmpc.org).

Results

Physiological and metabolic effects of methionine restriction (MetR) and cold exposure (CE)

To investigate the physiological impact of dietary sulfur amino acid content on EE under room temperature (RT, i.e., 22°C) and cold exposure (CE, 4°C for 24h), male C57BL/6N mice were placed one of three cysteine-depleted diets containing either 0.8% Methionine (Control; Ctrl), 0.12% Methionine (Methionine-restricted; MetR) or 2% Methionine (Methionine-supplemented; MetS) for six and five days, respectively (Fig 1A, i.e. study 1). Following the diet switch from housing diet to aforementioned experimental diets, EE increased progressively in the MetR group under RT conditions, rising from approx. 0.45 kcal/h to 0.6 kcal/h. Conversely, EE did not change in the Ctrl and MetS groups (Fig 1B). On day six, energy expenditure in the MetR group was significantly elevated compared to Ctrl and MetS groups, independent of starting bodyweight (Fig 1C, left). In contrast, CE elevated EE in all 3 diet groups to ~ 0.9 kcal/h, thereby rescinding the differences between MetR and the other two diets at RT (Fig 1A, 1C right, Fig S1A). MetR-fed animals exhibited significantly greater body weight loss compared to Ctrl and MetS-fed animals over the total duration of experimental diet feeding (Fig 1D). As food intake and locomotor activity were similar across groups (Fig S1B, S1D), the greater weight loss in MetR-fed animals is likely attributable to increased energy expenditure under RT conditions.

Consistent with previous studies, MetR feeding also increased water intake (Fig S1C). Respiratory exchange ratios (RER), as an indicator for macronutrient fuel selection, progressively increased during light and dark phases in the Ctrl and MetS groups, indicating enhanced carbohydrate utilization, whereas MetR-fed animals demonstrated lower RER indices, indicating a preference for lipid oxidation. Upon CE, RER decreased in Ctrl and MetS-fed animals to levels comparable to those observed in MetR-fed animals (Fig 1E, S1F). To further assess dietary and temperature interactions, we calculated daily averages of food and water intake, as well as locomotor activity and RER for each period. At RT, daily caloric intake was similar between groups and CE led to a consistent increase in caloric intake in all groups (Fig 1F). Average daily water intake was unaffected by ambient temperature, whereas daily locomotor activity exhibited a downward trend in all three groups during cold exposure (Fig 1F, Fig S1E). Collectively, these data demonstrate that short-term MetR increases energy expenditure by ca. 20% at RT and, as a consequence, promotes a metabolic shift toward lipid oxidation, potentially due to a transcriptional induction of thermogenic processes and/or lipolysis in catabolic adipose tissue depots such as iWAT or BAT. However, CE as

major physiological stimulus to induce non-shivering thermogenesis (NST) was able to override this MetR-induced effect, prompting an additional ca. 60% increase in EE independent of experimental diet feeding and body weight, alongside a shift to lipid utilization.

To further investigate the potential interactions between MetR- and CE-induced thermogenesis on physiological, metabolic and transcriptional parameters a second experiment was conducted: Here, mice were divided into four groups and either fed Ctrl or MetR diets (see study 1) for seven days at 22°C, or additionally exposed to 4°C for 24h (Study 2). In the following, animals fed Ctrl or MetR diets for 7 days at 22°C are denominated as Ctrl_RT and MetR_RT, while animals fed these diets for 7 days before being subjected to 24h of cold are denominated as Ctrl_CE and MetR_CE (Fig 1G). All groups experienced significant body weight loss during the intervention (Fig 1H), presumably due to single-housing. Counterintuitively, Ctrl_CE did not display exacerbated weight loss compared to the Ctrl_RT group. By contrast, MetR_RT led to approximately 10% body weight loss, and the combinational treatment (MetR_CE) resulted in further weight loss compared to MetR_RT alone (Fig 1H). The reductions in body weights coincided with organ-specific alterations in organ wet weights and organ/bodyweight ratios. Both Ctrl_CE and MetR_RT resulted in absolute (Fig 1I) and relative (Fig S1G) reductions in liver mass and MetR_CE reduced absolute and relative liver mass further in an additive fashion. The stepwise reduction in relative liver mass indicates that liver atrophy partly accounted for the observed body weight loss, predominantly in MetR-exposed mice. In contrast, Ctrl_CE alone did not affect iWAT, gWAT, or iBAT mass. Intriguingly, under MetR_RT all three adipose tissues showed (non-significant) upward trends in relative and absolute masses, which was exacerbated and partially significant under MetR_CE (Fig 1I, Fig S1G). Intriguingly, these data indicate that MetR_RT and Ctrl_CE synergize to promote increases adipose tissue mass particularly in gWAT and iBAT. To assess the associated systemic metabolic sequelæ of MetR- and CE , we measured circulating metabolic parameters: Blood glucose levels did not change significantly, but displayed a stepwise reduction between the groups, indicating additive effects between diet and ambient temperature (Fig 1J). In line with previous studies, serum triglyceride where reduced, albeit non-significantly, by Ctrl_CE and MetR_RT (19–21), but showed an even stronger reduction under MetR_CE, suggesting synergy (Fig 1J). By contrast, serum NEFA levels showed only minor non-significant reductions in both CE conditions and were unchanged by MetR_RT alone (Fig 1J), while serum beta-hydroxybutyrate levels, a marker of hepatic fatty acid oxidation, was elevated by either CE or

MetR feeding (Fig S1H). A major hormonal stimulus of EE in response to CE or MetR is mediated via 'thermogenic' hormones like FGF21 or IL-6. In line with the literature, Ctrl_CE and MetR_RT elevated circulating FGF21 levels even though the effect of cold was limited in this study. FGF21 levels did not further increase under MetR_CE, indicating that MetR maximally activates *Fgf21* transcription / FGF21 secretion to induce EE (Fig 1J). In contrast to literature, Ctrl_CE resulted in significant reductions in serum IL-6 levels in this study (Fig S1H) (22). MetR_RT also reduced serum IL-6 levels, with no further alterations under MetR_CE (Fig S1H). Together, these results suggest that while Cold exposure and MetR feeding individually trigger overlapping metabolic responses, their combination produces additive effects on weight loss, liver atrophy, and adipose size, alongside specific synergistic effects on triglyceride levels.

The transcriptional responses to CE and MetR-induced thermogenesis are tissue-specific

To investigate the transcriptional basis of the adaptation to two independent, yet potentially synergistic, physiological stimulators of NST, we next performed bulk mRNA-seq on liver, iBAT, iWAT, and eWAT across all four groups. Principal Component Analysis (PCA), as expected, revealed that the samples clustered according to their tissue of origin (Fig S2A). We next performed tissue-intrinsic PCA analyses that demonstrated highly tissue-specific responses (Fig 2A). (1) In the Liver, all 4 groups showed distinct transcriptional responses in PC1/2 whereas in (2) iBAT the groups clustered mostly by temperature (PC1), indicating that the transcriptional effects of MetR feeding are mild compared to CE. By contrast in both white adipose depots the 4 groups showed significant overlap although, in (3) iWAT, the clusters showed additive effects of MetR and CE along PC1, explaining 60% of the variation, while in (4) eWAT the clustered overlapped in PC1 and PC2. DEG analysis (adjusted pvalue < 0.05, $|FC| \geq 1.5$) showed that Ctrl_CE elicited stronger responses than MetR_RT in all tissues as exemplified by the higher number of differentially expressed genes without clear trends towards global transcriptional induction or repression. Of note, MetR was coupled to a higher number of repressed genes, potentially linked to the increased need for cellular energy conservation during amino acid-restriction. However, the combination of both stimuli elicited the strongest transcriptional responses in iWAT and eWAT (Fig 2B, S2B) and their interaction identified a high number of interacting genes, particularly in eWAT, cumulatively indicating that both stimuli cooperate to regulate gene transcription.

To understand to what degree the transcriptional responses are tissue / depot-specific or broadly applicable to all investigated organs, we analyzed the intersections between CE and

MetR in all four tissues (Fig 2C-F, S2C, D). Under Ctrl_CE and MetR_CE more than 50% of all DGE's were regulated in a tissue-specific manner in 3 out of the 4 tissues, with the most marked transcriptional effects seen in iWAT (Fig 2C-E). The degree of tissue-specific regulation was even higher in MetR_RT and in the interaction term (Fig 2D,F). Cumulatively, these data suggest that the majority of transcriptional effects of CE and dietary MetR are tissue-specific and display a varying degree of additive and synergistic effects.

To better scrutinise the individual transcriptional effects for each tissue, and to associate the observed gene-regulatory effects with cellular and metabolic processes, we next performed binary, combinatorial analyses of differential gene expression in liver (Fig 3), iBAT (Fig 4), iWAT (Fig 5) and eWAT (Fig 6) using similar in silico approaches.

CE drives gene induction while MetR and CE cooperatively repress genes in the liver

In the liver (Fig 3), this analysis revealed substantial gene regulation induced by Ctrl_CE (908 genes upregulated, 378 genes downregulated) and MetR_RT (272 genes upregulated, 432 genes downregulated), with even more genes regulated when combined under MetR_CE (829 genes upregulated, 721 genes downregulated). While Ctrl_CE appears to be a stronger stimulus based on the number of DEGs, MetR_RT appears to elicit stronger transcriptional effects based on log□FC (Fig 3A). Based on the number of DEGs, MetR_RT and Ctrl_CE, when combined under MetR_CE, appear to repress gene expression in an independent additive manner and induce genes in a dependent antagonistic manner (Fig 3A). Indeed only a limited number of genes were significant in diet × temperature interaction term (78 genes upregulated, 125 genes downregulated; Fig 3A) and the transcriptional effects of CE under MetR (MetR_CE vs MetR_RT) and MetR feeding under CE (MetR_CE vs Ctrl_CE) were lower compared to their respective counterparts (Fig S3A). To gain further insights into the degree of overlap between Ctrl_CE and MetR_RT, we performed Upset plot analysis. The biggest set of shared genes was found between Ctrl_CE and MetR_CE (517 DEGs), highlighting that Ctrl_CE is a major contributor to the transcriptional effects seen in MetR_CE (Fig 3B). While the direct of contribution of MetR_RT alone was lower (244 DEGs), this analysis also indicated a high degree of co-dependence on MetR_RT in the regulation of 505 DEGs in the MetR_CE condition, as well as the exclusion of 444 Ctrl_CE DEGs from the combined exposure (Fig 3B). Contrasting all MetR_CE DEGs between Ctrl_CE and MetR_RT ($R^2 = 0.39$), as well as contrasting all MetR_RT and Ctrl_CE DEGs ($R^2 = 0.31$) revealed relatively poor correlation between the respective log□FC values and suggests that the overall influence of Cold is stronger (Fig 3C, Fig S3B). We further

classified the regulation of all DEGs in the MetR_CE condition under consideration of significance, direction of regulation and interaction significance as proposed by García *et al.* (23). Co-dependent genes were significant only in MetR_CE but not in either stimuli alone. Concordant genes showed equal directional regulation in all three conditions, whereas Ctrl_CE or MetR_RT-dominant genes were significantly regulated in the under MetR_CE combination despite opposing or non-regulation in the other single exposure. The interaction of Ctrl_CE and MetR_RT was classified as additive if the gene was non-significant in the interaction term or, alternatively, classified as antagonistic/synergistic based on the direction of regulation. This analysis indicated that more than 50% of down-regulated genes were due to co-dependent additive regulation between Ctrl_CE and MetR_RT (brown) and MetR_RT alone (green). By contrast, more than 50% of the up-regulated genes were significant in the combined exposure due to Ctrl_CE (Fig 3D). Altogether, these data confirm Ctrl_CE drives the induction of genes, while Ctrl_CE and MetR_RT cooperate to repress genes under MetR_CE. Genes significant in either Ctrl_CE or MetR_RT but not in the combination Met_CE, were assigned as MetR_RT, Ctrl_CE, or mutually-masked in the same fashion as MetR_CE DEGs were previously assessed (Fig S3C). MetR_RT prevented a significant number of Ctrl_CE DEGs (n = 393 genes) from regulation under MetR_CE an additive (subtractive) fashion (Fig S3D). Finally, to understand which pathways are differentially regulated, we performed Gene set enrichment analysis (GSEA) under consideration of log□FC (24). Among the 20 most enriched pathways under MetR_CE, MetR drove the enrichment for metabolic pathways (Biosynthesis of amino acids, Glutathione or P450 cytochrome metabolism), while CE drove the enrichment in signaling pathways (cGMP-PKG, Glucagon and AMPK signaling) and Steroid biosynthesis (Fig 3F). These results are in line with previously published datasets (25,26). This analysis also revealed a number of gene sets where MetR_CE showed the highest enrichment, such as Glucagon signaling, TCA cycle, folate and amino acid biosynthesis. This indicates that MetR and CE cooperate in the regulation of gene sets related to energy provisioning and glucose metabolism in the liver (Fig 3F). The 20 most negatively enriched pathways feature many immune and disease-related gene sets (Fig S3D).

CE dominates gene induction in iBAT with limited contribution of MetR

In iBAT (Fig 4), volcano plot analysis revealed that Ctrl_CE elicited a stronger transcriptional response than MetR_RT (787 genes upregulated, 948 genes downregulated, versus 63 genes upregulated and 187 downregulated, respectively). The transcriptional

response to MetR_CE was only marginally larger (671 genes upregulated, 1114 genes downregulated), suggesting that the majority of the transcriptional response is driven by CE (Fig 4A). A small number of genes were identified in the diet × temperature interaction term (53 upregulated, 31 downregulated), indicating limited non-additive effects (Fig 4A), while CE on top of MetR (MetR_CE vs MetR_RT) still resulted in a similar magnitude in gene regulation as CE alone (Fig S4A). Upset plot analysis confirmed that the majority of DEGs in the combined MetR_CE condition overlapped with Ctrl_CE (1007 genes), while only a minor subset was shared with MetR_RT (88 genes; Fig 4B). Comparison of log□FC between Ctrl_CE and MetR_RT for all MetR_CE DEGs showed a weak correlation ($R^2 = 0.25$), supporting the notion that the transcriptional responses to MetR_CE are indeed driven by CE (Fig 4C). This weak correlation was confirmed when considering all MetR_RT or Ctrl_CE DEGs (Fig S4B). The classification of gene-regulation confirmed that >50% of down- and up-regulated genes were driven by Ctrl_CE (blue, Fig 4D). Altogether, these data indicate that Ctrl_CE primarily drives gene induction in iBAT, while the transcriptional effects of MetR_RT are negligible. GSEA analysis confirmed the positive enrichment of fatty acid and thermogenic pathways, as previously published (26,27). The combination of both stimuli specifically benefited the positive enrichment of metabolic pathways such as Fatty acid elongation and PPAR signaling, while Ctrl_CE drove the enrichment in ER and glycerolipid related gene sets. In line with the limited transcriptional response of MetR_RT on gene level, NES scores for MetR_RT were mostly lower compared to Ctrl_CE and/or non-significant. The few selected gene sets whose enrichment was driven by MetR_RT were Peroxisome and or Steriod biosynthesis (Fig 4E). In contrast, numerous immune-related pathways, including inflammatory bowel disease, cytokine signaling, and systemic lupus erythematosus, showed strong negative enrichment, indicating suppression of immune signaling. Interestingly, the enrichment of these pathways was dominated by MetR_RT (Fig S4D).

Additive and synergistic gene regulation by MetR and CE in iWAT

In iWAT (Fig 5), volcano plots revealed that both Ctrl_CE (1006 upregulated, 1392 genes downregulated) and MetR_RT (504 upregulated, 1037 downregulated) elicited marked transcriptional changes: The combination of both stimuli (MetR_CE) resulted in an even greater number of DEGs compared to either stimuli alone (1404 upregualted, 2266 downregulated), indicating either additive or synergistic effects (Fig 5A). Only a limited number of genes were identified in the diet × temperature interaction (118 down, 38 up), suggesting few non-additive responses (Fig 5A). Upset plots supported cooperativity between

MetR_RT and Ctrl_CE, with 1327 DGEs uniquely regulated when both stimuli were combined, but also supports true additive or synergistic regulation with 1115 genes being significantly regulated in all three conditions (Fig 5B). Correlation of log□FC between Ctrl_CE and MetR_RT for all MetR_CE showed a strong positive correlation ($R^2 = 0.79$), suggesting that the impact of Ctrl_CE and MetR_RT on gene regulation is similar in iWAT (Fig 5C, Fig S5B). Regulatory classification of DEGs revealed that both up- and down-regulated genes were predominantly regulated in an additive manner, where Ctrl_CE and MetR_RT cooperated to enhance transcriptional responses. This included genes that only became significant when both stimuli were combined (co-dependent regulation) as well as genes that were already significant under each condition but showed non-synergistic regulation under the combined treatment (concordant – additive; Fig 5D). GSEA analysis revealed significant enrichment in mostly positively regulated pathways and were consistent with expected CE- or MetR-induced responses, such as fatty acid degradation, PPAR signaling, thermogenesis, and the TCA cycle (Fig 5E) (26,27). Notably, nearly all of these pathways showed significant negative enrichment for the interaction term, indicating that the transcriptional response to MetR_CE is less than additive. This suggests that while both Ctrl_CE and MetR_RT independently activate key metabolic pathways, their combined effect is attenuated on the gene set level, possibly due to overlapping mechanisms or transcriptional feedback limiting further activation.

Codependent and synergistic gene regulation by MetR and CE in eWAT despite limited pathway activation

In eWAT (Fig 6), Volcano plot analysis revealed that both Ctrl_CE and MetR_RT alone did not have substantial effects on transcription, as less than 255 DEGs were up- or down-regulated in either condition (Fig 6A). This was in clear contrast to the combined effect under MetR_CE that featured 285 upregulated and 918 downregulated genes. The interaction term featured 496 DEGs, the highest among all tissues, suggesting a co-dependent and potentially synergistic mode of gene regulation under MetR_CE in eWAT. (Fig 6A). Upset plot analysis confirmed that most MetR_CE DEGs (856) are unique to the combination of CE and MetR, and that Ctrl_CE alone (54 DEGs) or MetR_RT alone (180 DEGs) contributed little to the joined MetR_CE effect (Fig 6B). A modest correlation in log□FC changes for all MetR_CE DEGs ($R^2 = 0.33$) or DEGs from either Ctrl_CE or MetR_RT ($R^2 = 0.33$), further supports the notion that Ctrl_CE and MetR_RT have disparate effects on gene regulation (Fig 6C,

S6B). To interrogate the regulatory logic, we examined the contribution of each stimulus to DEGs in the MetR_CE contrast, as stated previously. About 70% of all up- and down-regulated DEGs under MetR_CE were identified as co-dependent DEGs that became significant due to additive transcriptional effects of Ctrl_CE and MetR_RT (Fig 6D). The second biggest contributor to down-regulated DEGs was MetR_RT (MetR_RT–dominant - additive, green), while the remainder of the up-regulated genes are regulated through a mix of co-dependent synergistic, and Ctrl_CE or MetR_RT–dominant regulation (Fig 6D). Surprisingly, despite the cooperative notion in how Ctrl_CE and MetR_RT regulate gene expression under MetR_CE, GSEA yielded only a single negatively-enriched gene set for MetR_CE (motor proteins, not shown). This response was mirrored by MetR_RT which resulted in the enrichment of merely 3 gene sets (Circadian rhythm, Ribosome and Motor proteins, not shown). By contrast, Ctrl_CE resulted in the enrichment of 38 gene sets, which were all positively enriched. The top 20 gene sets for Ctrl_CE featured many gene sets relevant for energy metabolism (Oxidative phosphorylation, Thermogenesis, TCA cycle) and lipid handling (fatty acid metabolism, biosynthesis) (Fig 6E). In line with the lack of significant gene sets in MetR_RT or MetR_CE, NES scores for MetR_RT were all smaller compared to Ctrl_CE, and when combined (MetR_CE) resulted in negative NES scores (Fig 6E). These results suggest that while on gene level Ctrl_CE and MetR_RT amplify each other's transcriptional response, they antagonise each other functionally on the level of gene sets.

Discussion

In this work, we compared the systemic effects of two environmental stimuli of energy expenditure, dietary MetR and CE, in a 2x2 design, in order to assess whether both stimuli produce additively or synergistically steer systemic energy metabolism and transcriptional adaptation in key metabolic tissues. Our results indicate that although dietary MetR increases EE at RT and shifts substrate utilization toward lipid oxidation, CE constitutes a stronger stimulus for EE and masks diet-dependent differences. Combining CE and MetR resulted in mild reductions in bodyweight and glucose levels and additive reductions on circulating trigylceride levels and liver mass. Notwithstanding the threshold effects seen in the activation of FGF21 and beta-hydroxybutyrate (bOHB), markers for energy homeostasis and hepatic fatty acid oxdiation, respectively, these results suggest potential suitability of combining both stimuli for the correction of hyperglycemia, hypertriglyceridemia and excess bodyweight in disease settings.

To gain further insights into how MetR and CE converge on the transcriptional level we performed RNA-seq on liver, iBAT, iWAT and eWAT. We observed a high degree of depot-specificity in the transcriptional responses to MetR, CE and the combination, both on gene and pathway level. In liver, CE dominated gene induction while MetR and CE cooperatively repressed genes. The combination of both factors regulated pathways involved in energy and glucose handling (Glucagon signaling, TCA cycle, AMPK signaling, Amino acid & Carbon metabolism), potentially explaining the stepwise reduction in circulating glucose and triglyceride levels. In iBAT, CE dominated the transcriptional response, with limited contribution from MetR, and resulted in the enrichment of thermogenic and lipid-oxidation programs (thermogenesis, fatty acid metabolism). In iWAT, MetR and CE acted largely additively with high concordance, enhancing fatty-acid degradation, PPAR signaling, thermogenesis, and TCA cycle pathways. The transcriptional responses in eWAT was limited.

An intriguing finding of potential translational value was the cold-like transcriptional response elicited by MetR in iWAT. Amidst the emerging appreciation that the amount and metabolic activity of ‘classical’ human brown adipocytes might not contribute to overall EE and metabolic regulation in humans (28), other fat depots such as ‘beige’ subcutaneous adipose tissue (scWAT, i.e., the functional human equivalent to murine iWAT) are moving into the limelight of fundamental research and therapeutic pursuits (29). This is spurred by

the appreciation that human, just like rodent, white fat exerts important catabolic and endocrine functions (30), begetting the seminal question about the nature of physiological, pharmacological, dietary and lifestyle-associated interventions that will help achieve to increase energy dissipation via scWAT. Here, the unsolved task is to prompt uncoupling protein 1 (UCP1)-dependent and UCP1-independent biochemical processes such as Ca^{2+}/creatine cycling (31,32), or by inducing an energy-consuming combination of triacylglycerol breakdown and fatty acid re-esterification that occurs after sympathomimetic administration (33) selectively in beige fat. Intriguingly, a recent report demonstrated that oral supplementation of high-fat diet fed mice with a nitroalkene derivative of salicylate (SANA) can induce creatine cycling in rodent iWAT independent of UCP1, demonstrating that the activation of iWAT thermogenesis and mitochondrial respiration is exploitable using pharmacology. Noteworthy, a Phase 1 study demonstrated that human volunteers receiving SANA exhibited a modest degree of weight loss, suggesting that strategies for iWAT mobilisation in rodents might translate to (obese) patients (34). To date, orthogonal nutritional approaches for iWAT activation in mice rely on negative energy balances and include calorie restriction paradigms such as intermittent fasting (35), yet conclusive data on their effect in human scWAT remains limited (36,37) and might incur detrimental processes such as the unwanted mobilization of lean (muscle and bone) mass. The selective omission or removal of methionine and cysteine have proven to be efficient in activating EE via iWAT thermogenesis, and involve both humoral (FGF21 secretion) and sympathetic nervous system-dependent, UCP1-independent responses (26,38). Future studies with extended durations should clarify whether run-in dietary priming, e.g. via dietary MetR, can prime or enhance adaptive thermogenic responses during prolonged cold exposure, ideally monitored by continuous measurement of core body temperature and more in-depth molecular analysis of the browning phenotype in iWAT.

An intriguing opportunity for MetR might lie in maximising treatment effects against more clinical conditions ranging from cancer (39,40) to obesity. Here, drugs that mimic the action of the gut hormone glucagon-like peptide-1 (GLP1), i.e., so called GLP1 receptor agonists (GLP1Ra) such as semaglutide, have radically transformed obesity treatment and reduce body weight via reducing appetite (41). However, to date these drugs have the unfortunate downside of unfavorably reducing EE (42). As lead-in calorie restriction allows mice to maintain EE and thus enhance the degree of achievable weight loss (43), nutritional approaches might help to break the efficacy plateau that continue to plague GLP1Ras,

collectively highlighting the notion that dietary interventions such as selective amino acid restriction prior or during pharmacological treatment deserve further experimental exploration and clinical testing.

Classically, DIT is synonymous with the thermic effect of food (TEF) and describes the post-prandial rise in energy expenditure attributable to digestion, absorption, and metabolic processing of nutrients (44). This canonical, meal-linked DIT is transient and scales with meal energy composition (45). In contrast, MetR elevates EE independent of acute feeding by engaging an endocrine-neuronal axis, where hepatic amino-acid sensing activates the integrated stress response, increases FGF21 expression and circulating levels, and drives UCP1-dependent thermogenesis and beiging of WAT/BAT, thereby increasing EE (4,5). Related protein-restriction paradigms similarly raise EE through FGF21-mediated thermogenic programs (46). Our and previous data demonstrate that MetR increases EE at thermoneutral-adjacent conditions and elicits depot-specific thermogenic transcriptional programs, even when benchmarked against cold exposure. We propose that MetR represents a true form of “diet-induced thermogenesis” in a mechanistic sense i.e., a diet composition-initiated, hormone-driven thermogenic state that is distinct from the classic meal-processing TEF.

Our study provides important initial insights into depot-specific transcriptional responses to MetR, CE, and their combination, yet several limitations remain. The relatively short duration (7 days MetR, 24-hour CE) was sufficient for assessing acute transcriptional interactions but limited our ability to investigate long-term physiological adaptations or sustained metabolic remodeling. Furthermore, applying complementary omics analyses, including proteomics and metabolomics or flux analysis would provide deeper mechanistic insights into metabolic interactions at the protein and metabolite levels.

Figure legends:

Figure 1. Physiological and metabolic effects of methionine restriction (MetR) and cold exposure (CE). (A) Schematic depicting 11 day experimental setup and dietary composition for mouse experiment 1. (B) Energy expenditure (EE) over the entire experiment duration. (C) ANCOVA analysis of average nighttime EE on days 6 and 11 over body weight. (D) Bodyweight and body weight loss (%). (E) Respiratory exchange ratio (RER) over the entire experiment duration. (F) Average daily food and water intake over all RT (22 °C) or CE (4 °C) experimental days. (G) Schematic depicting 8 day experimental setup for mouse experiment 2. Dietary compositions for Ctrl and MetR diets are the same as in mouse experiment 1. Groups are denominated as Ctrl_RT, Ctrl_CE, MetR_RT and MetR_CE. (H) Bodyweight and body weight loss (%). (I) Absolute organ weights for Liver, inguinal WAT, gonadal WAT, interscapular BAT. Statistics were done within tissues. (J) Blood glucose, serum triglycerides, and FGF21 levels. EE was analyzed by ANCOVA using body weight as a covariate (via mmpc.org); p-values were Bonferroni-corrected. Bodyweight, average food and water intake were analyzed via two-way ANOVA with *p□<□0.05, **p□<□0.01, ***p□<□0.001, ****p□<□0.0001. Body Weight loss, serum parameters and absolute organ weights were analyzed using one-way ANOVA with Tukey's post hoc test. Different letters indicate statistically significant differences (p□<□0.05).

Figure 2. The transcriptional responses to Cold exposure (CE) and MetR-induced thermogenesis are tissue-specific. (A) Tissue-specific PCA plots for Liver, iBAT, iWAT, and eWAT. (B) Number of differentially expressed genes (DEGs), split into induced (red) and repressed (blue) genes, per contrast (adjusted p-value < 0.05, |FC| > 1.5). (C-F) UpSet plots showing overlap of DEGs across tissues for each contrast: (C) Ctrl_CE vs Ctrl_RT, (D) MetR_RT vs Ctrl_RT, (E) MetR_CE vs Ctrl_RT, and (F) Interaction. Set size bars indicate the total number of DEGs per tissue; intersection bars indicate the number of shared DEGs between tissues. Dots and bars in orange represent tissue-specific DEGs.

Figure 3. Cold exposure (CE) drives gene induction while methionine restriction (MetR) and CE cooperatively repress genes in the liver. (A) Volcano plots showing DEGs for each contrast (Ctrl_CE vs Ctrl_RT, MetR_RT vs Ctrl_RT, MetR_CE vs Ctrl_RT, and the diet × temperature interaction). Numbers indicate significantly up- and downregulated genes

(adjusted p-value < 0.05, |FC| > 1.5). (B) Upset plot showing the overlap of DEGs across contrasts. Intersection bars indicate the number of shared DEGs between contrasts. Dots in orange represent contrast-specific DEGs. (C) Scatter plot of log□FC values in Ctrl_CE vs Ctrl_RT and MetR_RT vs Ctrl_RT for DEGs from the MetR_CE condition. n denominates DEGs shown. (D) Schematic highlighting gene expression profiles. Arrows indicate significant regulation for induced (up; red) or repressed (down; blue) genes. Non-significant regulation is depicted as grey dots. (E) Classification of MetR_CE DEGs based on their mode of regulation mode. (F) GSEA of the top 20 positively enriched pathways in MetR_CE vs Ctrl_RT. Dot size represents gene ratio, color denotes contrast, and significance is indicated by filled circles (adjusted p-value < 0.05).

Figure 4. CE dominates gene induction in iBAT with limited contribution of MetR (A) Volcano plots showing DEGs for each contrast (Ctrl_CE vs Ctrl_RT, MetR_RT vs Ctrl_RT, MetR_CE vs Ctrl_RT, and the diet × temperature interaction). Numbers indicate significantly up- and downregulated genes (adjusted p-value < 0.05, |FC| > 1.5). (B) Upset plot showing the overlap of DEGs across contrasts. Intersection bars indicate the number of shared DEGs between contrasts. Dots in orange represent contrast-specific DEGs. (C) Scatter plot of log□FC values in Ctrl_CE vs Ctrl_RT and MetR_RT vs Ctrl_RT for DEGs from the MetR_CE condition. n denominates DEGs shown. (D) Classification of MetR_CE DEGs based on their mode of regulation mode. (E) GSEA of the top 20 positively enriched pathways in MetR_CE vs Ctrl_RT. Dot size represents gene ratio, color denotes contrast, and significance is indicated by filled circles (adjusted p-value < 0.05).

Figure 5. Additive and synergistic gene regulation by MetR and CE in iWAT (A) Volcano plots showing DEGs for each contrast (Ctrl_CE vs Ctrl_RT, MetR_RT vs Ctrl_RT, MetR_CE vs Ctrl_RT, and the diet × temperature interaction). Numbers indicate significantly up- and downregulated genes (adjusted p-value < 0.05, |FC| > 1.5). (B) Upset plot showing the overlap of DEGs across contrasts. Intersection bars indicate the number of shared DEGs between contrasts. Dots in orange represent contrast-specific DEGs. (C) Scatter plot of log□FC values in Ctrl_CE vs Ctrl_RT and MetR_RT vs Ctrl_RT for DEGs from the MetR_CE condition. n denominates DEGs shown. (D) Classification of MetR_CE DEGs based on their mode of regulation mode. (E) GSEA of the top 20 positively enriched

pathways in MetR_CE vs Ctrl_RT. Dot size represents gene ratio, color denotes contrast, and significance is indicated by filled circles (adjusted p-value < 0.05).

Figure 6. Codependent and synergistic gene regulation by MetR and CE in eWAT despite limited pathway activation (A) Volcano plots showing DEGs for each contrast (Ctrl_CE vs Ctrl_RT, MetR_RT vs Ctrl_RT, MetR_CE vs Ctrl_RT, and the diet × temperature interaction). Numbers indicate significantly up- and downregulated genes (adjusted p-value < 0.05, |FC| > 1.5). (B) Upset plot showing the overlap of DEGs across contrasts. Intersection bars indicate the number of shared DEGs between contrasts. Dots in orange represent contrast-specific DEGs. (C) Scatter plot of log□FC values in Ctrl_CE vs Ctrl_RT and MetR_RT vs Ctrl_RT for DEGs from the MetR_CE condition. n denominates DEGs shown. (D) Classification of MetR_CE DEGs based on their mode of regulation mode. (E) GSEA of the top 20 positively enriched pathways in MetR_CE vs Ctrl_RT. Dot size represents gene ratio, color denotes contrast, and significance is indicated by filled circles (adjusted p-value < 0.05). Supplementary figure legends:

Supplemental figure 1. (A) ANCOVA analysis of average nighttime EE on days 6 and 11 over average nighttime locomotor activity. (B) Cumulative food intake (kcal) over the entire study period. (C) Cumulative water intake (mL) over the entire study period. (D) Cumulative locomotor activity (beam breaks) over the entire study period. (E) Average daily locomotor activity over all RT (22 °C) or CE (4 °C) experimental days. (F) Average light and dark phase RER at days 4-6 (RT) and days 9-11 (CE). (G) Relative organ weights for liver, iWAT, gWAT, iBAT. Statistics were done within tissues. (H) Serum beta-hydroxybutyrate (bOHB), Non-esterified fatty acids (NEFA) and IL-6 levels. EE was analyzed by ANCOVA using average locomotor activity as a covariate (via mmpc.org); p-values were Bonferroni-corrected. Average daily locomotor activity, and average RER were analyzed via two-way ANOVA with *p□<□0.05, **p□<□0.01, ***p□<□0.001, ****p□<□0.0001. Serum parameters and relative organ weights were analyzed using one-way ANOVA with with Tukey's post hoc test. Different letters indicate statistically significant differences (p□<□0.05).

Supplemental figure 2. (A) PCA plot of all RNA-seq samples colored by tissue and shaped by experimental group. (B) Number of DEGs (adjusted p-value < 0.05, |FC| > 1.5) in each tissue across the indicated comparisons, split into up- (red) and down- (blue) regulated genes. (C-D) UpSet plots showing overlap of DEGs across tissues for each contrast: (C) MetR_CE vs MetR_RT, (D) MetR_CE vs Ctrl_CE. Set size bars indicate the total number of DEGs per tissue; intersection bars indicate the number of shared DEGs between tissues. Dots and bars in orange represent tissue-specific DEGs.

Supplementary Figure 3. (A) Volcano plots showing DEGs for MetR_CE vs MetR_RT (left) and MetR_CE vs Ctrl_CE (right). Numbers indicate significantly up- and downregulated genes (adjusted p-value < 0.05, |FC| > 1.5). (B) Scatter plot comparing log□FC values in Ctrl_CE vs Ctrl_RT and MetR_RT vs Ctrl_RT for DEGs significant in either condition. Colored dots indicate DEGs specific to each contrast or MetR_CE. n denominates DEGs shown. (C) Schematic highlighting gene expression profiles. Arrows indicate significant regulation for induced (up; red) or repressed (down; blue) genes. Non-significant regulation is depicted as grey dots. (D) Regulation classification of DEGs found in Ctrl_CE vs Ctrl_RT (left) or MetR_RT vs Ctrl_RT (right), but not MetR_CE vs Ctrl_RT. (E) GSEA for the top 20 negatively enriched pathways in the MetR_CE vs Ctrl_RT comparison. Dot size reflects gene ratio, colors indicate contrast group, and significance is shown by filled circles. While many pathways are regulated in individual contrasts, some interaction-specific pathways are evident, particularly among immune-related processes.

Supplementary Figure 4. (A) Volcano plots showing DEGs for MetR_CE vs MetR_RT (left) and MetR_CE vs Ctrl_CE (right). Numbers indicate significantly up- and downregulated genes (adjusted p-value < 0.05, |FC| > 1.5). (B) Scatter plot comparing log□FC values in Ctrl_CE vs Ctrl_RT and MetR_RT vs Ctrl_RT for DEGs significant in either condition. Colored dots indicate DEGs specific to each contrast or MetR_CE. n denominates DEGs shown. (C) Regulation classification of DEGs found in Ctrl_CE vs Ctrl_RT (left) or MetR_RT vs Ctrl_RT (right), but not MetR_CE vs Ctrl_RT. (D) GSEA for the top 20 negatively enriched pathways in the MetR_CE vs Ctrl_RT comparison. Dot size reflects gene ratio, colors indicate contrast group, and significance is shown by filled circles.

While many pathways are regulated in individual contrasts, some interaction-specific pathways are evident, particularly among immune-related processes.

Supplementary Figure 5. (A) Volcano plots showing DEGs for MetR_CE vs MetR_RT (left) and MetR_CE vs Ctrl_CE (right). Numbers indicate significantly up- and downregulated genes (adjusted p-value < 0.05, |FC| > 1.5). (B) Scatter plot comparing log□FC values in Ctrl_CE vs Ctrl_RT and MetR_RT vs Ctrl_RT for DEGs significant in either condition. Colored dots indicate DEGs specific to each contrast or MetR_CE. n denominates DEGs shown. (C) Regulation classification of DEGs found in Ctrl_CE vs Ctrl_RT (left) or MetR_RT vs Ctrl_RT (right), but not MetR_CE vs Ctrl_RT. (D) GSEA for the top 20 negatively enriched pathways in the MetR_CE vs Ctrl_RT comparison. Dot size reflects gene ratio, colors indicate contrast group, and significance is shown by filled circles. While many pathways are regulated in individual contrasts, some interaction-specific pathways are evident, particularly among immune-related processes.

Supplementary Figure 6. (A) Volcano plots showing DEGs for MetR_CE vs MetR_RT (left) and MetR_CE vs Ctrl_CE (right). Numbers indicate significantly up- and downregulated genes (adjusted p-value < 0.05, |FC| > 1.5). (B) Scatter plot comparing log□FC values in Ctrl_CE vs Ctrl_RT and MetR_RT vs Ctrl_RT for DEGs significant in either condition. Colored dots indicate DEGs specific to each contrast or MetR_CE. n denominates DEGs shown. (C) Regulation classification of DEGs found in Ctrl_CE vs Ctrl_RT (left) or MetR_RT vs Ctrl_RT (right), but not MetR_CE vs Ctrl_RT. (D) GSEA for the top 20 negatively enriched pathways in the MetR_CE vs Ctrl_RT comparison. Dot size reflects gene ratio, colors indicate contrast group, and significance is shown by filled circles. While many pathways are regulated in individual contrasts, some interaction-specific pathways are evident, particularly among immune-related processes.

References

1. Phelps NH, Singleton RK, Zhou B, Heap RA, Mishra A, Bennett JE, et al. Worldwide trends in underweight and obesity from 1990 to 2022: a pooled analysis of 3663 population-representative studies with 222 million children, adolescents, and adults. The Lancet. 2024 Mar;403(10431):1027–50.

2. Schlein C, Heeren J. Implications of thermogenic adipose tissues for metabolic health. Best Pract Res Clin Endocrinol Metab. 2016 Aug;30(4):487–96.

3. Yoneshiro T, Aita S, Matsushita M, Kayahara T, Kameya T, Kawai Y, et al. Recruited brown adipose tissue as an antiobesity agent in humans. J Clin Invest. 2013 Aug;123(8):3404–8.

4. Fang H, Stone KP, Wanders D, Forney LA, Gettys TW. The Origins, Evolution, and Future of Dietary Methionine Restriction. Annu Rev Nutr. 2022 Aug 22;42:201–26.

5. Forney LA, Fang H, Sims LC, Stone KP, Vincik LY, Vick AM, et al. Dietary Methionine Restriction Signals to the Brain Through Fibroblast Growth Factor 21 to Regulate Energy Balance and Remodeling of Adipose Tissue. Obes Silver Spring Md. 2020 Oct;28(10):1912–21.

6. Wanders D, Burk DH, Cortez CC, Van NT, Stone KP, Baker M, et al. UCP1 is an essential mediator of the effects of methionine restriction on energy balance but not insulin sensitivity. FASEB J Off Publ Fed Am Soc Exp Biol. 2015 Jun;29(6):2603–15.

7. Babygirija R, Lamming DW. The regulation of healthspan and lifespan by dietary amino acids. Transl Med Aging. 2021;5:17–30.

8. Wanders D, Forney LA, Stone KP, Burk DH, Pierse A, Gettys TW. FGF21 Mediates the Thermogenic and Insulin-Sensitizing Effects of Dietary Methionine Restriction but Not Its Effects on Hepatic Lipid Metabolism. Diabetes. 2017 Apr;66(4):858–67.

9. Spann RA, Morrison CD, den Hartigh LJ. The Nuanced Metabolic Functions of Endogenous FGF21 Depend on the Nature of the Stimulus, Tissue Source, and Experimental Model. Front Endocrinol. 2021;12:802541.

10. Mudge JM, Carbonell-Sala S, Diekhans M, Martinez JG, Hunt T, Jungreis I, et al. GENCODE 2025: reference gene annotation for human and mouse. Nucleic Acids Res. 2025 Jan 6;53(D1):D966–75.

11. Dobin A, Davis CA, Schlesinger F, Drenkow J, Zaleski C, Jha S, et al. STAR: ultrafast universal RNA-seq aligner. Bioinforma Oxf Engl. 2013 Jan 1;29(1):15–21.

12. Liao Y, Smyth GK, Shi W. featureCounts: an efficient general purpose program for assigning sequence reads to genomic features. Bioinforma Oxf Engl. 2014 Apr 1;30(7):923–30.

13. Patro R, Duggal G, Love MI, Irizarry RA, Kingsford C. Salmon provides fast and bias-aware quantification of transcript expression. Nat Methods. 2017 Apr;14(4):417–9.

14. Soneson C, Love MI, Robinson MD. Differential analyses for RNA-seq: transcript-level estimates improve gene-level inferences. F1000Research. 2015;4:1521.

15. Love MI, Huber W, Anders S. Moderated estimation of fold change and dispersion for RNA-seq data with DESeq2. Genome Biol. 2014;15(12):550.

16. Zhu A, Ibrahim JG, Love MI. Heavy-tailed prior distributions for sequence count data: removing the noise and preserving large differences. Bioinforma Oxf Engl. 2019 Jun 1;35(12):2084–92.

17. Yu G, Wang LG, Han Y, He QY. clusterProfiler: an R package for comparing biological themes among gene clusters. Omics J Integr Biol. 2012 May;16(5):284–7.

18. Davidsen LI, Hagberg CE, Goitea V, Lundby SM, Larsen S, Ebbesen MF, et al. Mouse vascularized adipose spheroids: an organotypic model for thermogenic adipocytes. Front Endocrinol. 2024;15:1396965.

19. Grefhorst A, Van Den Beukel JC, Dijk W, Steenbergen J, Voortman GJ, Leeuwenburgh S, et al. Multiple effects of cold exposure on livers of male mice. J Endocrinol. 2018 Aug;238(2):91–106.

20. Hasek BE, Boudreau A, Shin J, Feng D, Hulver M, Van NT, et al. Remodeling the Integration of Lipid Metabolism Between Liver and Adipose Tissue by Dietary Methionine Restriction in Rats. Diabetes. 2013 Oct 1;62(10):3362–72.

21. Bartelt A, Bruns OT, Reimer R, Hohenberg H, Ittrich H, Peldschus K, et al. Brown adipose tissue activity controls triglyceride clearance. Nat Med. 2011 Feb;17(2):200–5.

22. Bal NC, Maurya SK, Pani S, Sethy C, Banerjee A, Das S, et al. Mild cold induced thermogenesis: are BAT and skeletal muscle synergistic partners? Biosci Rep. 2017 Oct 31;37(5):BSR20171087.

23. Pantaleón García J, Kulkarni VV, Reese TC, Wali S, Wase SJ, Zhang J, et al. OBIF: an omics-based interaction framework to reveal molecular drivers of synergy. NAR Genomics Bioinforma. 2022 Jun;4(2):lqac028.

24. Subramanian A, Tamayo P, Mootha VK, Mukherjee S, Ebert BL, Gillette MA, et al. Gene set enrichment analysis: a knowledge-based approach for interpreting genome-wide expression profiles. Proc Natl Acad Sci U S A. 2005 Oct 25;102(43):15545–50.

25. Zhang Z, Cheng L, Ma J, Wang X, Zhao Y. Chronic Cold Exposure Leads to Daytime Preference in the Circadian Expression of Hepatic Metabolic Genes. Front Physiol. 2022;13:865627.

26. Ghosh S, Forney LA, Wanders D, Stone KP, Gettys TW. An integrative analysis of tissue-specific transcriptomic and metabolomic responses to short-term dietary methionine restriction in mice. PloS One. 2017;12(5):e0177513.

27. Hao Q, Yadav R, Basse AL, Petersen S, Sonne SB, Rasmussen S, et al. Transcriptome profiling of brown adipose tissue during cold exposure reveals extensive regulation of glucose metabolism. Am J Physiol Endocrinol Metab. 2015 Mar 1;308(5):E380-392.

28. Becher T, Palanisamy S, Kramer DJ, Eljalby M, Marx SJ, Wibmer AG, et al. Brown adipose tissue is associated with cardiometabolic health. Nat Med. 2021 Jan;27(1):58–65.

29. Sun W, Modica S, Dong H, Wolfrum C. Plasticity and heterogeneity of thermogenic adipose tissue. Nat Metab. 2021 Jun;3(6):751–61.

30. Blondin DP. Human thermogenic adipose tissue. Curr Opin Genet Dev. 2023 Jun;80:102054.

31. Rahbani JF, Roesler A, Hussain MF, Samborska B, Dykstra CB, Tsai L, et al. Creatine kinase B controls futile creatine cycling in thermogenic fat. Nature. 2021 Feb;590(7846):480–5.

32. Ikeda K, Kang Q, Yoneshiro T, Camporez JP, Maki H, Homma M, et al. UCP1-independent signaling involving SERCA2b-mediated calcium cycling regulates beige fat thermogenesis and systemic glucose homeostasis. Nat Med. 2017 Dec;23(12):1454–65.

33. Blondin DP, Nielsen S, Kuipers EN, Severinsen MC, Jensen VH, Miard S, et al. Human Brown Adipocyte Thermogenesis Is Driven by β2-AR Stimulation. Cell Metab. 2020 Aug 4;32(2):287-300.e7.

34. Cal K, Leyva A, Rodríguez-Duarte J, Ruiz S, Santos L, Garat MP, et al. A nitroalkene derivative of salicylate, SANA, induces creatine-dependent thermogenesis and promotes weight loss. Nat Metab. 2025 Jun 17;

35. Li G, Xie C, Lu S, Nichols RG, Tian Y, Li L, et al. Intermittent Fasting Promotes White Adipose Browning and Decreases Obesity by Shaping the Gut Microbiota. Cell Metab. 2017 Oct 3;26(4):672-685.e4.

36. Roth CL, Molica F, Kwak BR. Browning of White Adipose Tissue as a Therapeutic Tool in the Fight against Atherosclerosis. Metabolites. 2021 May 14;11(5):319.

37. Plummer JD, Johnson JE. Intermittent methionine restriction reduces IGF-1 levels and produces similar healthspan benefits to continuous methionine restriction. Aging Cell. 2022 Jun;21(6):e13629.

38. Lee AH, Orliaguet L, Youm YH, Maeda R, Dlugos T, Lei Y, et al. Cysteine depletion triggers adipose tissue thermogenesis and weight loss. Nat Metab. 2025 Jun;7(6):1204–22.

39. Gao X, Sanderson SM, Dai Z, Reid MA, Cooper DE, Lu M, et al. Dietary methionine influences therapy in mouse cancer models and alters human metabolism. Nature. 2019 Aug;572(7769):397–401.

40. Sanderson SM, Gao X, Dai Z, Locasale JW. Methionine metabolism in health and cancer: a nexus of diet and precision medicine. Nat Rev Cancer. 2019 Nov;19(11):625–37.

41. Müller TD, Blüher M, Tschöp MH, DiMarchi RD. Anti-obesity drug discovery: advances and challenges. Nat Rev Drug Discov. 2022 Mar;21(3):201–23.

42. Löffler MC, Betz MJ, Blondin DP, Augustin R, Sharma AK, Tseng YH, et al. Challenges in tackling energy expenditure as obesity therapy: From preclinical models to clinical application. Mol Metab. 2021 Sep;51:101237.

43. Petersen J, Merrild C, Lund J, Holm S, Clemmensen C. Lead-in calorie restriction enhances the weight-lowering efficacy of incretin hormone-based pharmacotherapies in mice. Mol Metab. 2024 Nov;89:102027.

44. Calcagno M, Kahleova H, Alwarith J, Burgess NN, Flores RA, Busta ML, et al. The Thermic Effect of Food: A Review. J Am Coll Nutr. 2019 Aug;38(6):547–51.

45. Swaminathan R, King RF, Holmfield J, Siwek RA, Baker M, Wales JK. Thermic effect of feeding carbohydrate, fat, protein and mixed meal in lean and obese subjects. Am J Clin Nutr. 1985 Aug;42(2):177–81.

46. Laeger T, Henagan TM, Albarado DC, Redman LM, Bray GA, Noland RC, et al. FGF21 is an endocrine signal of protein restriction. J Clin Invest. 2014 Sep;124(9):3913–22.

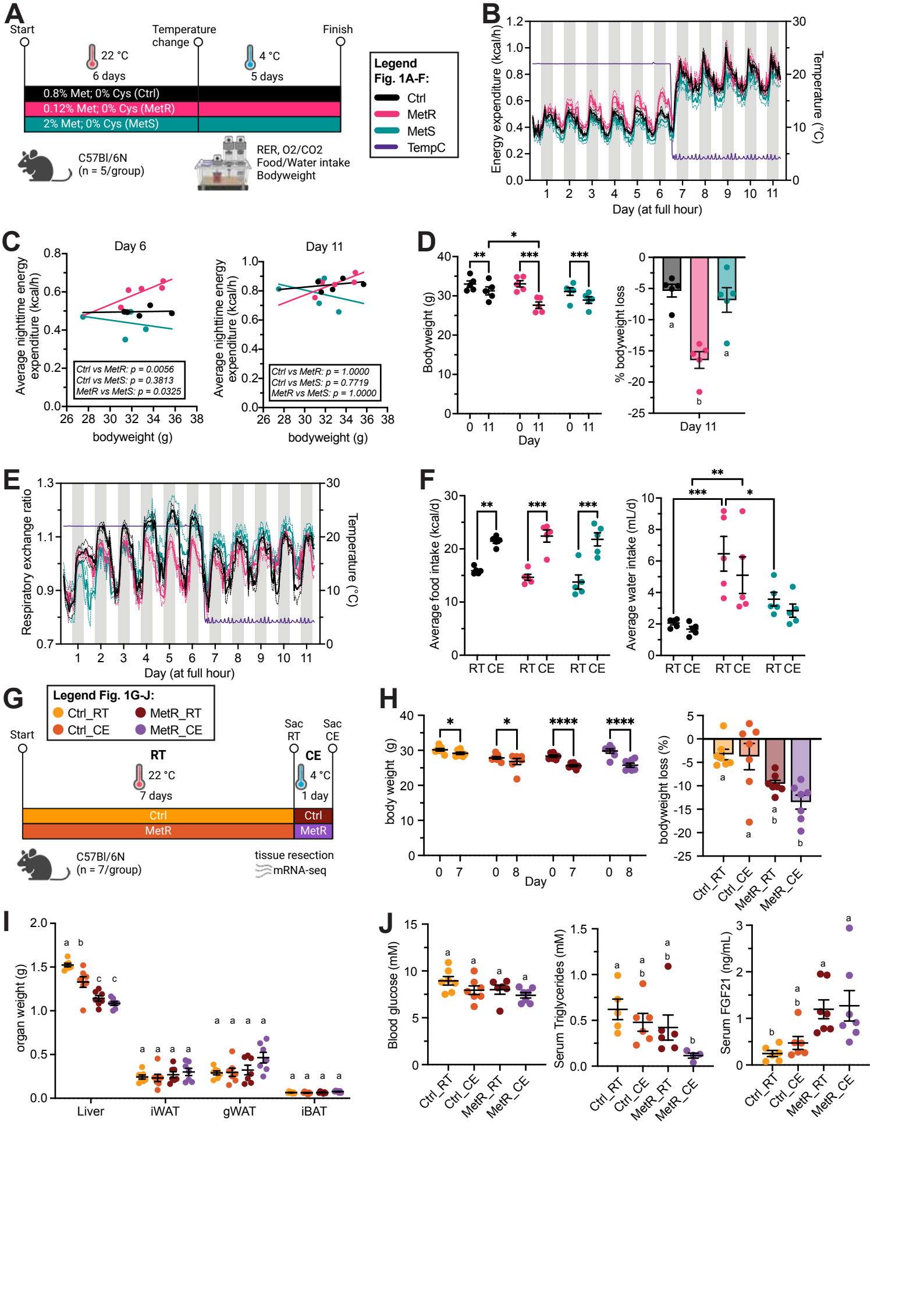
A
Start
Temperature change
Finish
22 °C
6 days
4 °C
5 days
0.8% Met; 0% Cys (Ctrl)
0.12% Met; 0% Cys (MetR)
2% Met; 0% Cys (MetS)
C57Bl/6N
(n = 5/group)
RER, O2/CO2
Food/Water intake
Bodyweight
Legend
Fig. 1A-F:
Ctrl
MetR
MetS
TempC
B
Energy expenditure (kcal/h)
Temperature (°C)
Day (at full hour)
C
Day 6
Day 11
Average nighttime energy expenditure (kcal/h)
bodyweight (g)
Ctrl vs MetR: p = 0.0056
Ctrl vs MetS: p = 0.3813
MetR vs MetS: p = 0.0325
Ctrl vs MetR: p = 1.0000
Ctrl vs MetS: p = 0.7719
MetR vs MetS: p = 1.0000
D
Bodyweight (g)
Day
% bodyweight loss
Day 11
E
Respiratory exchange ratio
Temperature (°C)
Day (at full hour)
F
Average food intake (kcal/d)
Average water intake (mL/d)
RT CE
G
Legend Fig. 1G-J:
Ctrl_RT
Ctrl_CE
MetR_RT
MetR_CE
Start
Sac RT
Sac CE
RT
22 °C
7 days
CE
4 °C
1 day
Ctrl
MetR
C57Bl/6N
(n = 7/group)
tissue resection
mRNA-seq
H
body weight (g)
Day
bodyweight loss (%)
Ctrl_RT
Ctrl_CE
MetR_RT
MetR_CE
I
organ weight (g)
Liver
iWAT
gWAT
iBAT
J
Blood glucose (mM)
Serum Triglycerides (mM)
Serum FGF21 (ng/mL)

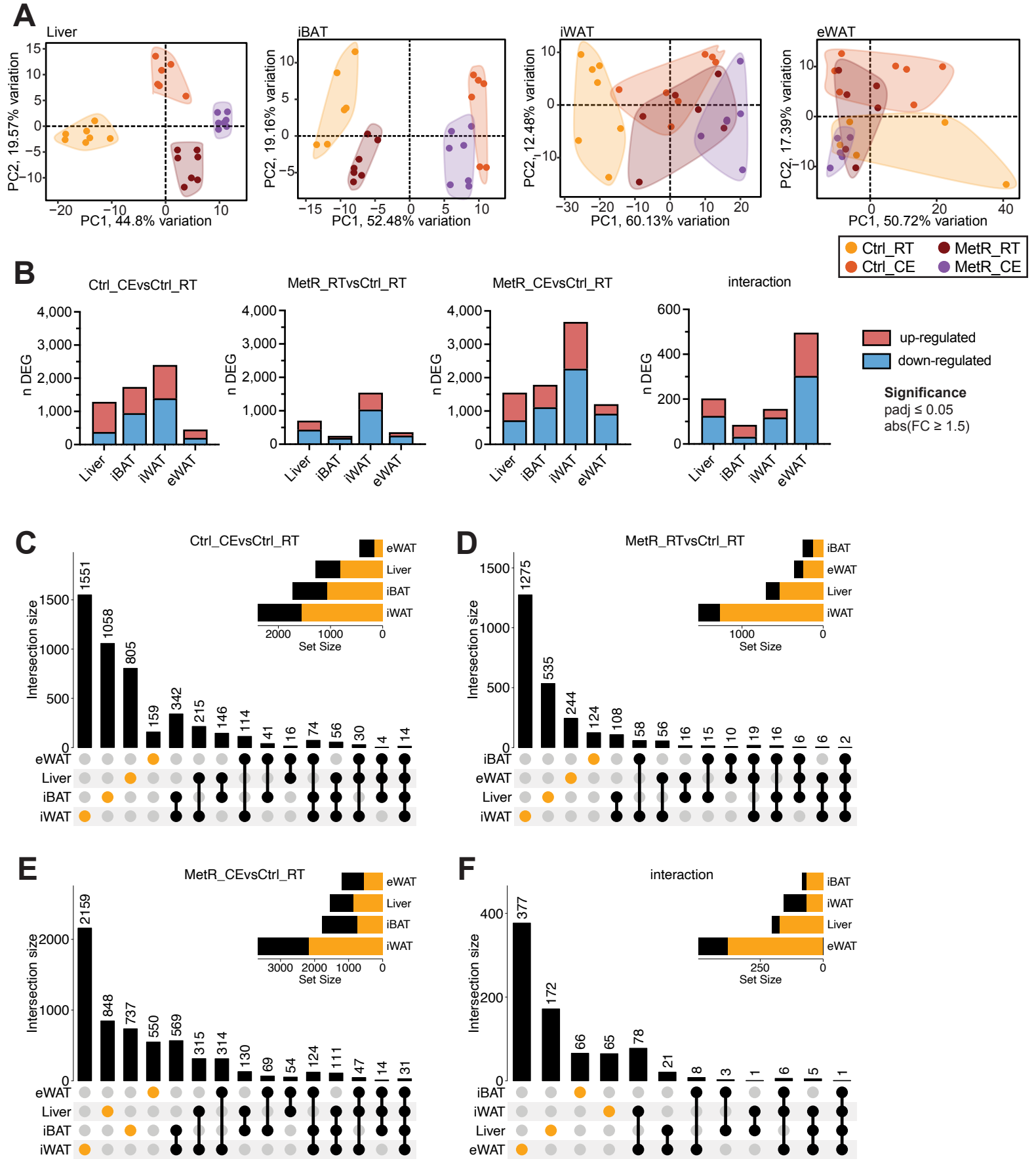
A
Liver
iBAT
iWAT
eWAT
PC2, 19.57% variation
PC1, 44.8% variation
PC2, 19.16% variation
PC1, 52.48% variation
PC2, 12.48% variation
PC1, 60.13% variation
PC2, 17.39% variation
PC1, 50.72% variation
Ctrl_RT
Ctrl_CE
MetR_RT
MetR_CE
B
Ctrl_CEvsCtrl_RT
MetR_RTvsCtrl_RT
MetR_CEvsCtrl_RT
interaction
n DEG
Liver
iBAT
iWAT
eWAT
up-regulated
down-regulated
Significance
padj ≤ 0.05
abs(FC ≥ 1.5)
C
Ctrl_CEvsCtrl_RT
Intersection size
Set Size
1551
1058
805
159
342
215
146
114
41
16
74
56
30
4
14
D
MetR_RTvsCtrl_RT
1275
535
244
124
108
58
56
16
15
10
19
16
6
6
2
E
MetR_CEvsCtrl_RT
2159
848
737
550
569
315
314
130
69
54
124
111
47
14
31
F
interaction
377
172
66
65
78
21
8
3
1
6
5
1

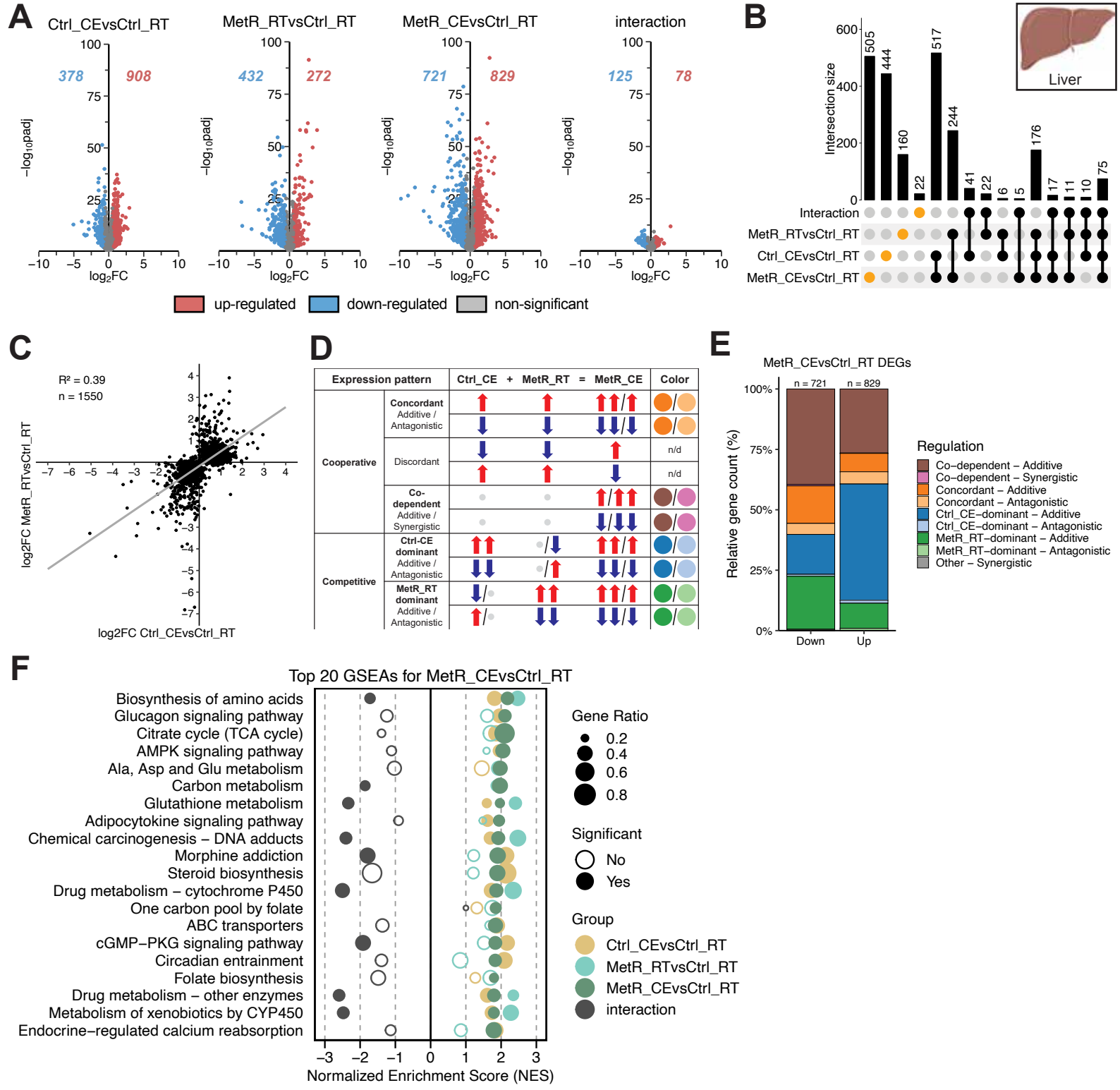
A
Ctrl_CEvsCtrl_RT
MetR_RTvsCtrl_RT
MetR_CEvsCtrl_RT
interaction
378
908
432
272
721
829
125
78
−log10padj
log2FC
up-regulated
down-regulated
non-significant
B
Liver
Intersection size
505
444
160
22
517
244
41
22
6
5
176
17
11
10
75
Interaction
MetR_RTvsCtrl_RT
Ctrl_CEvsCtrl_RT
MetR_CEvsCtrl_RT
C
R² = 0.39
n = 1550
log2FC MetR_RTvsCtrl_RT
log2FC Ctrl_CEvsCtrl_RT
D
Expression pattern
Ctrl_CE + MetR_RT = MetR_CE
Color
Cooperative
Concordant Additive / Antagonistic
Discordant
n/d
Co-dependent Additive / Synergistic
Competitive
Ctrl-CE dominant Additive / Antagonistic
MetR_RT dominant Additive / Antagonistic
E
MetR_CEvsCtrl_RT DEGs
n = 721
n = 829
Relative gene count (%)
Down
Up
Regulation
Co−dependent − Additive
Co−dependent − Synergistic
Concordant − Additive
Concordant − Antagonistic
Ctrl_CE−dominant − Additive
Ctrl_CE−dominant − Antagonistic
MetR_RT−dominant − Additive
MetR_RT−dominant − Antagonistic
Other − Synergistic
F
Top 20 GSEAs for MetR_CEvsCtrl_RT
Biosynthesis of amino acids
Glucagon signaling pathway
Citrate cycle (TCA cycle)
AMPK signaling pathway
Ala, Asp and Glu metabolism
Carbon metabolism
Glutathione metabolism
Adipocytokine signaling pathway
Chemical carcinogenesis − DNA adducts
Morphine addiction
Steroid biosynthesis
Drug metabolism − cytochrome P450
One carbon pool by folate
ABC transporters
cGMP−PKG signaling pathway
Circadian entrainment
Folate biosynthesis
Drug metabolism − other enzymes
Metabolism of xenobiotics by CYP450
Endocrine−regulated calcium reabsorption
Normalized Enrichment Score (NES)
Gene Ratio
0.2
0.4
0.6
0.8
Significant
No
Yes
Group
Ctrl_CEvsCtrl_RT
MetR_RTvsCtrl_RT
MetR_CEvsCtrl_RT
interaction

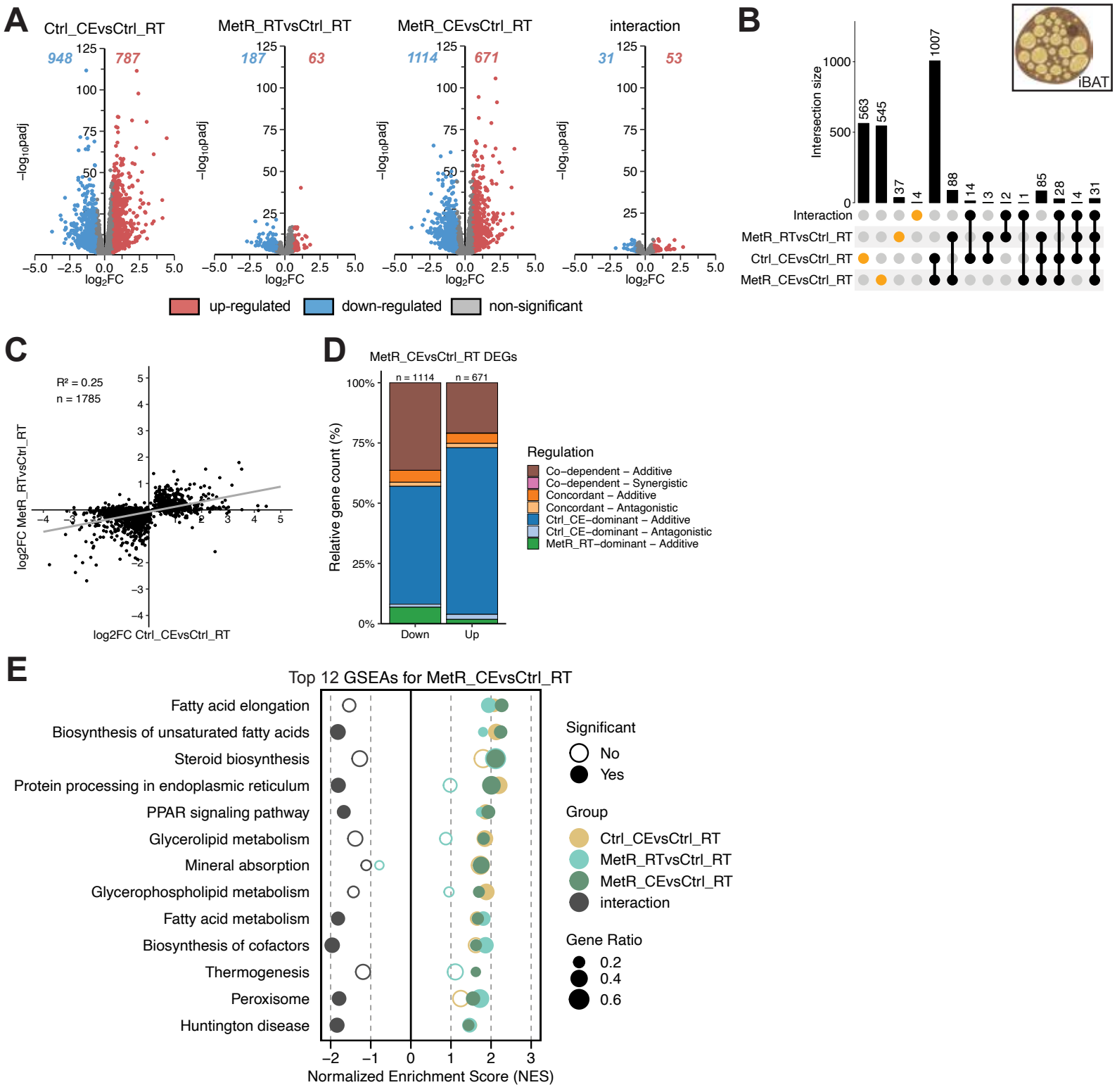
A
Ctrl_CEvsCtrl_RT
948
787
MetR_RTvsCtrl_RT
187
63
MetR_CEvsCtrl_RT
1114
671
interaction
31
53
−log10padj
log2FC
up-regulated
down-regulated
non-significant
B
iBAT
Intersection size
563
545
37
4
1007
88
14
3
2
1
85
28
4
31
Interaction
MetR_RTvsCtrl_RT
Ctrl_CEvsCtrl_RT
MetR_CEvsCtrl_RT
C
R² = 0.25
n = 1785
log2FC MetR_RTvsCtrl_RT
log2FC Ctrl_CEvsCtrl_RT
D
MetR_CEvsCtrl_RT DEGs
n = 1114
n = 671
Relative gene count (%)
Down
Up
Regulation
Co−dependent − Additive
Co−dependent − Synergistic
Concordant − Additive
Concordant − Antagonistic
Ctrl_CE−dominant − Additive
Ctrl_CE−dominant − Antagonistic
MetR_RT−dominant − Additive
E
Top 12 GSEAs for MetR_CEvsCtrl_RT
Fatty acid elongation
Biosynthesis of unsaturated fatty acids
Steroid biosynthesis
Protein processing in endoplasmic reticulum
PPAR signaling pathway
Glycerolipid metabolism
Mineral absorption
Glycerophospholipid metabolism
Fatty acid metabolism
Biosynthesis of cofactors
Thermogenesis
Peroxisome
Huntington disease
Normalized Enrichment Score (NES)
Significant
No
Yes
Group
Ctrl_CEvsCtrl_RT
MetR_RTvsCtrl_RT
MetR_CEvsCtrl_RT
interaction
Gene Ratio
0.2
0.4
0.6

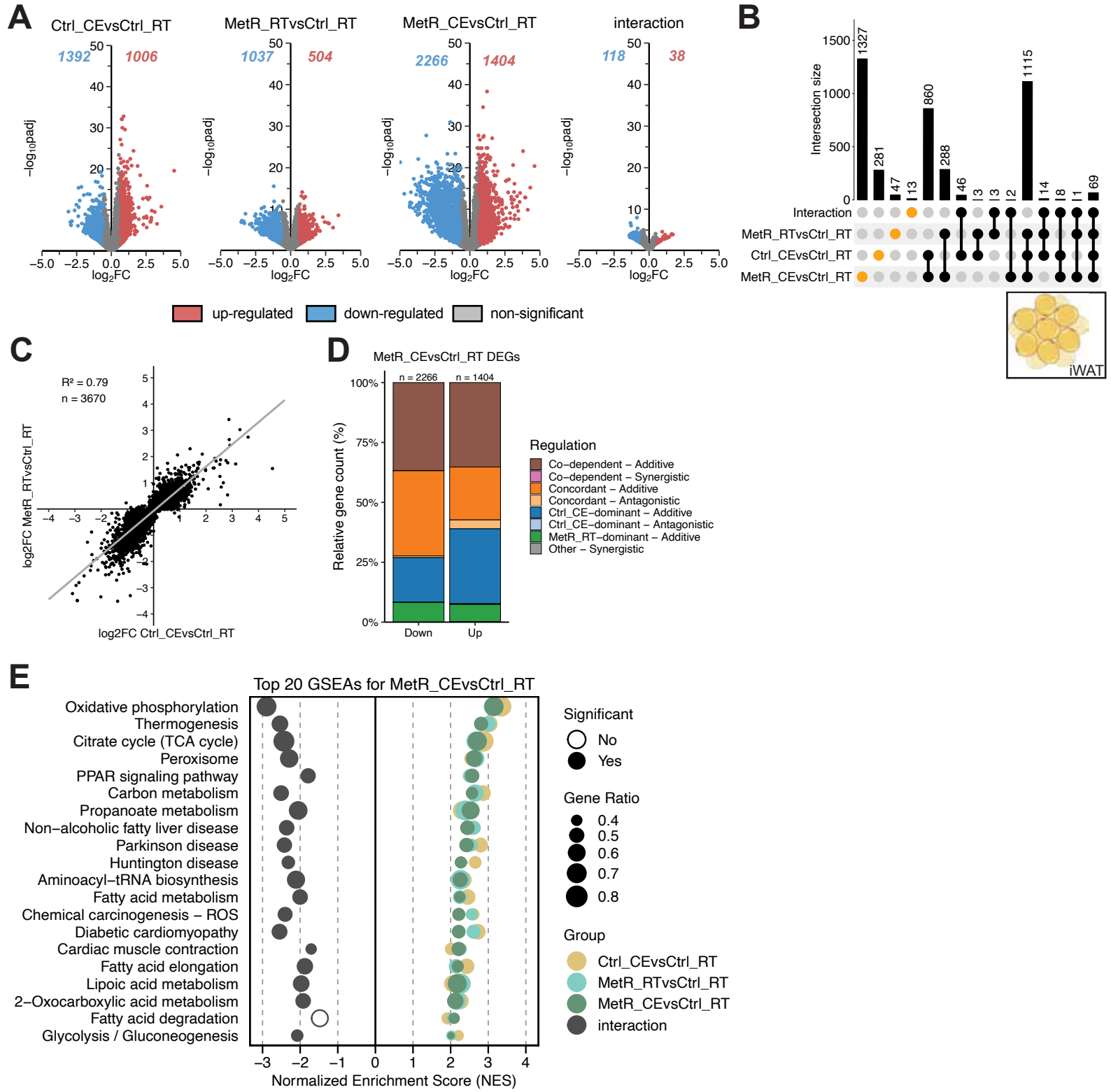
A
Ctrl_CEvsCtrl_RT
1392
1006
MetR_RTvsCtrl_RT
1037
504
MetR_CEvsCtrl_RT
2266
1404
interaction
118
38
−log10padj
log2FC
up-regulated
down-regulated
non-significant
B
Intersection size
1327
281
47
13
860
288
46
3
3
2
1115
14
8
1
69
Interaction
MetR_RTvsCtrl_RT
Ctrl_CEvsCtrl_RT
MetR_CEvsCtrl_RT
iWAT
C
R² = 0.79
n = 3670
log2FC MetR_RTvsCtrl_RT
log2FC Ctrl_CEvsCtrl_RT
D
MetR_CEvsCtrl_RT DEGs
n = 2266
n = 1404
Relative gene count (%)
Down
Up
Regulation
Co−dependent − Additive
Co−dependent − Synergistic
Concordant − Additive
Concordant − Antagonistic
Ctrl_CE−dominant − Additive
Ctrl_CE−dominant − Antagonistic
MetR_RT−dominant − Additive
Other − Synergistic
E
Top 20 GSEAs for MetR_CEvsCtrl_RT
Oxidative phosphorylation
Thermogenesis
Citrate cycle (TCA cycle)
Peroxisome
PPAR signaling pathway
Carbon metabolism
Propanoate metabolism
Non−alcoholic fatty liver disease
Parkinson disease
Huntington disease
Aminoacyl−tRNA biosynthesis
Fatty acid metabolism
Chemical carcinogenesis − ROS
Diabetic cardiomyopathy
Cardiac muscle contraction
Fatty acid elongation
Lipoic acid metabolism
2−Oxocarboxylic acid metabolism
Fatty acid degradation
Glycolysis / Gluconeogenesis
Normalized Enrichment Score (NES)
Significant
No
Yes
Gene Ratio
0.4
0.5
0.6
0.7
0.8
Group
Ctrl_CEvsCtrl_RT
MetR_RTvsCtrl_RT
MetR_CEvsCtrl_RT
interaction

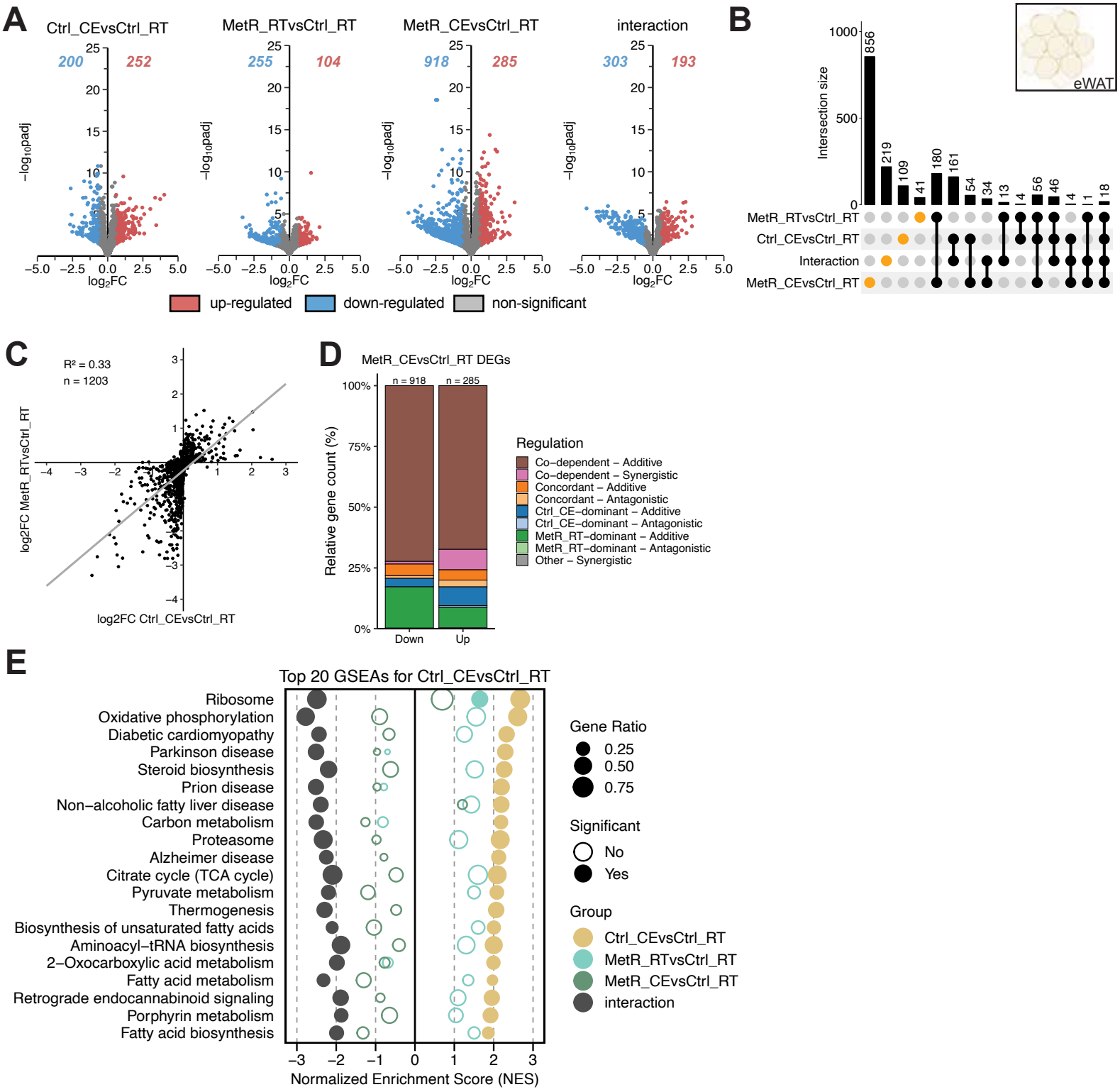
A
Ctrl_CEvsCtrl_RT
200
252
MetR_RTvsCtrl_RT
255
104
MetR_CEvsCtrl_RT
918
285
interaction
303
193
−log10padj
log2FC
up-regulated
down-regulated
non-significant
B
eWAT
Intersection size
856
219
109
41
180
161
54
34
13
4
56
46
4
1
18
MetR_RTvsCtrl_RT
Ctrl_CEvsCtrl_RT
Interaction
MetR_CEvsCtrl_RT
C
R² = 0.33
n = 1203
log2FC MetR_RTvsCtrl_RT
log2FC Ctrl_CEvsCtrl_RT
D
MetR_CEvsCtrl_RT DEGs
n = 918
n = 285
Relative gene count (%)
Down
Up
Regulation
Co−dependent − Additive
Co−dependent − Synergistic
Concordant − Additive
Concordant − Antagonistic
Ctrl_CE−dominant − Additive
Ctrl_CE−dominant − Antagonistic
MetR_RT−dominant − Additive
MetR_RT−dominant − Antagonistic
Other − Synergistic
E
Top 20 GSEAs for Ctrl_CEvsCtrl_RT
Ribosome
Oxidative phosphorylation
Diabetic cardiomyopathy
Parkinson disease
Steroid biosynthesis
Prion disease
Non−alcoholic fatty liver disease
Carbon metabolism
Proteasome
Alzheimer disease
Citrate cycle (TCA cycle)
Pyruvate metabolism
Thermogenesis
Biosynthesis of unsaturated fatty acids
Aminoacyl−tRNA biosynthesis
2−Oxocarboxylic acid metabolism
Fatty acid metabolism
Retrograde endocannabinoid signaling
Porphyrin metabolism
Fatty acid biosynthesis
Normalized Enrichment Score (NES)
Gene Ratio
0.25
0.50
0.75
Significant
No
Yes
Group
Ctrl_CEvsCtrl_RT
MetR_RTvsCtrl_RT
MetR_CEvsCtrl_RT
interaction